HHS Public Access

Author manuscript

Matrix Biol. Author manuscript; available in PMC 2020 January 01.

Published in final edited form as:

Matrix Biol. 2019 January ; 75-76: 314–330. doi:10.1016/j.matbio.2018.06.004.

CD44-dependent inflammation, fibrogenesis, and collagenolysis regulates extracellular matrix remodeling and tensile strength during cutaneous wound healing

Priya Govindaraju[1,2], **Leslie Todd**[1], **Snehal Shetye**[3], **James Monslow**[1], and **Ellen Puré**[1,2]

[1]Department of Biomedical Sciences of the University of Pennsylvania, Philadelphia, PA

[2]Pharmacology Graduate Group of the University of Pennsylvania, Philadelphia, PA

[3]McKay Orthopaedic Research Laboratory of the University of Pennsylvania, Philadelphia, PA

Abstract

Cutaneous wound healing consists of three main phases: inflammation, re-epithelialization, and tissue remodeling. During normal wound healing, these processes are tightly regulated to allow restoration of skin function and biomechanics. In many instances, healing leads to an excess accumulation of fibrillar collagen (the principal protein found in the extracellular matrix - ECM), and the formation of scar tissue, which has compromised biomechanics, tested using ramp to failure tests, compared to normal skin [1], Alterations in collagen accumulation and architecture have been attributed to the reduced tensile strength found in scar tissue [2,3]. Defining mechanisms that govern cellular functionality and ECM remodeling are vital to understanding normal versus pathological healing and developing approaches to prevent scarring. CD44 is a cell surface adhesion receptor expressed on nearly all cell types present in dermis. Although CD44 has been implicated in an array of inflammatory and fibrotic processes such as leukocyte recruitment, T-cell extravasation, and hyaluronic acid (the principal glycosaminoglycan found in the ECM) metabolism, the role of CD44 in cutaneous wound healing and scarring remains unknown. We demonstrate that in an excisional biopsy punch wound healing model, CD44-null mice have increased inflammatory and reduced fibrogenic responses during early phases of wound healing. At wound closure, CD44-null mice exhibit reduced collagen degradation leading to increased accumulation of fibrillar collagen, which persists after wound closure leading to reduced tensile strength resulting in a more severe scarring phenotype compared to WT mice. These data indicate that CD44 plays a previously unknown role in fibrillar collagen accumulation and wound healing during the injury response.

Keywords

Cutaneous wound healing; fibrillar collagen; activated fibroblasts; scar tissue

Corresponding Author: Ellen Puré, epure@upenn.edu, University of Pennsylvania, 380 S. University Avenue, Hill Pavilion 410E, Philadelphia, PA 19104.

Introduction

The densely packed connective tissue in the dermis, consisting primarily of fibrillar collagen, impacts the elasticity and tensile strength characteristic of normal skin. Upon tissue injury an orchestrated set of events is initiated to prevent infection and repair wounded tissue. Mammalian fetal wounds are adept at regenerative wound healing and can therefore restore tissue integrity, biomechanics, and function. Mammalian adult wounds are notoriously unable to regenerate and instead, wounded tissue is replaced by scar tissue. Scars are characterized by an excess accumulation of fibrillar collagen, prolonged inflammation, and/or impaired neovascularization. Increased synthesis, accumulation and/or crosslinking of fibrillar collagen, comprised of type I and type III collagen, is associated with compromised tensile strength and hence tissue function [4–9], Although various biochemical and biomechanical processes have been hypothesized to play a role in wound healing, there is still a significant gap in understanding regulators of normal versus aberrant cutaneous wound healing.

CD44, a transmembrane cell adhesion receptor widely expressed on most cell types present in the dermis, plays vital roles in cell-cell and cell-matrix interactions, particularly under pathophysiologic conditions. Its primary ligand, hyaluronic acid (HA), is the predominant glycosaminoglycan found in the extracellular matrix (ECM) and is prevalent through all phases of the wound response [10,11], CD44 plays a critical role in retention of HA on the cell surface and also mediates HA endocytosis [12,13], In addition to its role as an HA receptor, CD44 also co-localizes with matrix metalloproteinase-9 (MMP-9), vascular endothelial growth factor (VEGF), epidermal growth factor (EGF), fibronectin, type I collagen, and osteopontin [14–21], *In vitro* studies have shown that CD44 is critical for MMP-dependent transforming growth factor-beta (TGF-β) activation, directional fibroblast migration, stiffness-dependent fibroblast motility but not proliferation, nor fibroblast invasion and adhesion to a provisional fibrin-rich matrix [22–24], *In vivo* studies have shown CD44 upregulation following tissue injury [25–28].

In an ischemic cardiac injury model, CD44-null fibroblasts demonstrated reduced fibroblast infiltration and collagen accumulation [29]; however, in an acute lung injury model, CD44-null mice showed no significant changes in collagen accumulation [30,31], Conversely, CD44-null mice exhibited attenuated atherosclerosis due to decreased recruitment of macrophages, regulation of vascular smooth muscle cells (VSMC) proliferation and increased fibrous cap formation [25,32]. Although CD44 has been studied in various fibrotic diseases, the role of CD44 in regulating collagen biosynthesis and turnover remains unknown.

To determine if CD44 plays a role in collagen accumulation and scar tissue formation, we studied the impact of genetic CD44 deletion in a full-thickness excisional cutaneous wound healing model. Given that CD44 has been shown to play vital roles in recruitment, activation, and clearance of cells from sites of tissue injury, we analyzed cellular and matrix composition of wounds over the course of and post wound resolution. Our results indicate that during early response to injury, CD44-null mice exhibit a reduced fibrogenic but an

increased inflammatory response. During tissue restoration, CD44-null mice demonstrated reduced collagenolysis leading to increased collagen accumulation and compromised tissue biomechanics.

Results

CD44 deficiency alters the kinetics of fibrillar collagen accumulation during cutaneous wound healing

Cutaneous wound healing occurs in three main stages: inflammatory, re-epithelialization, and tissue remodeling [6]. During early stages of wound healing, the granulation tissue is comprised of a provisional matrix, including high levels of fibronectin (FN), HA, and type III collagen, which is vital for cellular adhesion and migration to the granulation tissue [6,33–35], During the tissue remodeling phase, there is an increase in type I collagen accumulation, which is crucial for regaining tissue elasticity and strength. Aberrant ECM accumulation and architecture is indicative of pathological wound healing with excess scar formation.

At baseline, CD44-null mice demonstrated normal skin histology, collagen content (measured by quantification of masson's trichrome and picrosirius red staining visualized under circular polarized light), HA (measured by ELISA) and stromal cell content (based on quantification of percent positive cells and levels of expression of $CD90^+$, fibroblast activation protein (FAP^+) and/or alpha-smooth muscle actin (αSMA^+) cells quantified by flow cytometry) compared to WT mice (Fig. S1A – I).

We investigated the impact of CD44 on wound healing by comparing the response to full thickness excisional wounds (6 mm in diameter) generated 4 mm below the shoulder blades on the dorsal side of the skin using biopsy punches, in WT and CD44-null mice. Wounds were kept hydrated using tegaderm (bandages) and curad (tape) to minimize scab formation [36] (Fig. 1A). The rate of wound closure was measured by quantification of digital images captured on days 1, 3, 5, 7, 9, and 11 post-wounding. The kinetics of wound closure were comparable in WT and CD44-null mice (Fig. 1B) with both genotypes exhibiting complete re-epithelialization and wound closure by day 11. Morphometric analysis of sections revealed no significant differences in total cellularity days 5, 7 and 11 post-wounding, measured using DAPI nuclear stain, and area of granulation tissue visualized by H&E staining at wound closure (Fig. S2A, B).

The role of CD44 in matrix accumulation and remodeling during cutaneous wound healing was investigated by comparing ECM composition, organization and architecture in WT and CD44-null mice at days 5, 7 and 11 post-wounding. During early phases of wound healing (days 5 and 7), wounds from CD44-null mice had reduced type I collagen (measured using immunofluorescence), and fibrillar collagen (measured using two-photon second harmonic generation imaging - 2P-SHG) compared to WT mice (Fig. 1C,D). However, at wound closure (day 11) CD44-null mice exhibited greater accumulation of type I collagen and fibrillar collagen compared to WT mice (Fig. 1C,D). CD44-null mice did not show any significant differences in accumulation of HA (Fig. S3A) or FN at any time point during the wound healing response when compared to WT mice (Fig. S3B). These results indicate that

in response to injury, CD44 plays a role in matrix remodeling by regulating fibrillar collagen accumulation.

CD44 deficiency enhances leukocyte but attenuates FAP$^+$ fibroblast accumulation during early phases of wound healing

Wound healing is the result of a coordinated multistep cascade of events involving inflammatory cells, endothelial cells, keratinocytes and fibroblasts. The inflammatory response initiated upon tissue injury plays a vital role in the release of cytokines and growth factors involved in fibroblast recruitment, activation, and consequent ECM deposition [37–39], In several models of tissue injury CD44 was shown to be required for leukocyte recruitment, adhesion, and clearance. In contrast however, in a lung injury model CD44 deletion enhanced neutrophil recruitment suggesting that CD44 can limit recruitment of neutrophils in particular settings [30,40–42], Given this cell-type and context-dependent role of CD44 in regulating the inflammatory/immune response, we next investigated the impact of CD44 deletion on the inflammatory/immune response during cutaneous wound repair. We analyzed infiltration by total leukocyte, neutrophils, T cells, M1 and M2 macrophages days 5, 7 and 11 post-wounding. During early phases of wound healing (days 5 and 7), perhaps surprisingly, we found that CD44-null wounds had increased numbers of total leukocytes as measured using the pan-leukocyte marker CD45$^+$ (Fig. S4A). Further analysis revealed that no specific immune cell population was altered including neutrophils (CD11b$^+$ Ly6G$^+$), M1 macrophages (F4/80$^+$ iNOS$^+$), M2 macrophages (F4/80$^+$CD206$^+$), and T cells (CD3$^+$) in CD44-null wounds (Fig. S4B – E) that collectively accounted for the overall increase in CD45$^+$ leukocytes. To determine the impact of increased leukocytes on the inflammatory milieu during early phases of wound healing, levels of cytokines implicated in wound healing including IL-1β, IL-4, TNF-α, and IL-10 were analyzed using ELISAs [43–46], Consistent with the observed increase in leukoctyes during early phases of wound healing, we found increased levels of IL-1β and IL-4 day 5 post-wounding in CD44-null wounds compared to WT wounds (Fig. S4 F, G). These increases were selective in that CD44-null wounds showed no significant differences in TNF-α, and IL-10 levels day 5 post-wounding (Fig. S4 H, I). Additionally, despite a significant increase in number of leukocytes, no significant differences in expression levels of cytokines were found in WT and CD44-null wounds day 7 post-wounding (Fig. S4 F – I). These data suggests that at day 7 post-wounding, the increase in leukocytes in CD44-null wounds is not sufficient to alter cytokine levels or that additional cell types, including fibroblasts, may compensate for the increase in leukocytes in CD44-null wounds compared to WT wounds.

The initial inflammatory phase of wound repair is followed by recruitment, proliferation, and activation of fibroblasts [4–6], Fibroblasts are a heterogeneous cell population responsible for matrix production and remodeling [47,48], α-SMA is a canonical marker of myofibroblasts that are involved in wound contraction, as well as tissue fibrosis. In epithelial tumors, pulmonary fibrosis, liver cirrhosis and myocardial infarction, fibroblast activation protein (FAP) identifies distinct, yet to varying degrees, overlapping subsets of activated fibroblasts [49–54], We recently demonstrated that FAP$^+$ and α-SMA$^+$ fibroblasts exhibit distinct gene expression patterns and divergent functions *in vitro* [48], Based on these findings, we conducted immunohistochemistry (IHC) on serial sections of wounds days 5, 7

and 11 post-wounding for vimentin (mesenchymal cell marker), FAP, and α-SMA to analyze the spatial and temporal distribution of total mesenchymal cells as well as these distinct activated fibroblast subsets over the course of wound healing. Interestingly, we found that in WT wounds, vimentin$^+$ and α-SMA$^+$ fibroblasts gradually increased over the course of wound closure, whereas FAP$^+$ fibroblasts were prevalent early and remained relatively constant (Fig. 2A-D). These data provide key evidence for temporal regulation of different mesenchymal cell subsets during cutaneous wound healing. Compared to WT wounds, CD44-null wounds showed no significant differences in the temporal profile of vimentin$^+$ and α-SMA$^+$ fibroblasts (Fig. 2A-C), but exhibited a marked delay in the kinetics of FAP$^+$ fibroblasts accumulation. Specifically, during early phases of wound healing (days 5 and 7) CD44-null wounds had a significant reduction in FAP$^+$ fibroblasts compared to WT wounds (Fig. 2A, 2D), which was overcome by the time of wound closure, providing evidence for CD44 dependent temporal regulation of FAP$^+$ fibroblasts.

These mesenchymal cells also exhibited interesting differences in their spatial distributions. At day 5 post-wounding, vimentin$^+$, FAP$^+$, and α-SMA$^+$ cells were all concentrated at the wound edge and proximal to the hypodermis region in both WT and CD44-null wounds (Fig. 2A; top panel). By day 7 post-wounding, vimentin$^+$fibroblasts were found dispersed throughout the granulation tissue while the α-SMA$^+$ cells remained mainly at the wound edge in both genotypes. Interestingly, we distribution of FAP+ cells diverged in wounds in WT vs CD44-null mice by day 7. Specifically, in WT wounds, FAP$^+$ fibroblasts showed a similar distribution pattern to vimentin$^+$ fibroblasts throughout the granulation tissue but in wounds in CD44-null mice FAP$^+$ cells were primarily present proximal to the hypodermis region (Fig. 2A; middle panel). At wound closure (day 11), vimentin$^+$ fibroblasts remained dispersed throughout the granulation tissue in both genotypes. While FAP$^+$ cells were mainly concentrated proximal to the hypodermis region, α-SMA$^+$ cells were present throughout the granulation tissue and proximal to the epidermis (Fig. 2A; lower panel) in both WT and CD44-null wounds. This indicated that CD44 regulates both spatial and temporal distribution of FAP$^+$ reactive fibroblasts during early phases of wound healing.

CD44 deficiency reduces collagenolysis activity during cutaneous wound healing

Fibrillar collagen biosynthesis involves synthesis of pro-α chains, hydroxylation of proline and lysine residues, inter- and intra-molecular crosslinking, and assembly into fibrils [55,56], Following incorporation into the extracellular matrix, collagen metabolism occurs by extracellular proteolysis (by collagenases and gelatinases) followed by cellular uptake and lysosomal degradation [57].

To identify the role of CD44 in collagen metabolism resulting in increased accumulation at wound closure, a biochemical analysis of collagen was conducted day 11 post-wounding. CD44-null wounds showed no difference in content of hydroxylated proline residues or in mRNA levels for lysl oxidase (lox), an enzyme involved in collagen crosslinking, compared to WT wounds (Fig. S5A – B). CD44-null wounds also showed no significant differences in protein levels for Endo180, a receptor involved in cellular uptake/lysosomal degradation of collagen, when compared to WT wounds (Fig. S5C – D). *In situ* zymography however demonstrated reduced collagenase activity during early phases of wound healing and at

wound closure, days 7 and 11, in CD44-null compared to WT wounds (Fig. 3A). CD44-null wounds also had reduced gelatinase activity during early phases of wound healing but not at wound closure (Fig. 3B).

Fibroblast CD44-dependent collagenolysis regulates fibrillar collagen accumulation *in vitro*

To determine the mechanism by which CD44 regulates fibrillar collagen accumulation, we utilized a fibroblast-derived matrix (FDM) approach [58], WT and CD44-null dermal fibroblasts from naïve unwounded skin were cultured for 8 days on cross-linked gelatin coated plates in the presence of 75 μg/ml of ascorbic acid - an essential cofactor of collagen lysl and prolyl hydroxylation and facilitates the formation of the collagen triple helix [59]. CD44-null fibroblasts showed no difference in cell viability (Fig. S6A), measured by calcein AM, total and activated fibroblast markers (Fig. S6B), based on flow cytometric analysis for CD90, FAP, and α-SMA, and lox mRNA levels (Fig. S6C) compared to WT fibroblasts *in vitro.*

Analogous to day 11 wounds, analysis of collagen from WT and CD44-null FDMs showed no differences in hydroxylated proline residues (Fig. S6D). On the 8th day of matrix production, a detergent treatment was used to decellularize matrices, which were then analyzed using 2P-SHG for fibrillar collagen accumulation. Analogous to day 11 wounds, FDMs derived from CD44-null fibroblasts contained greater fibrillar collagen accumulation compared to WT fibroblasts (Fig. 4A).

Quantification of MMP mRNA levels using qPCR, revealed no significant differences in MMP levels between WT and CD44-null fibroblasts depositing FDMs. To identify if CD44 plays a role in MMP activity, WT and CD44-null fibroblasts depositing matrices were supplemented 20 μg/ml of DQ collagen 24 hours prior to decellularization. DQ collagen is a collagen analog with excessive fluorescein labeling in close proximity resulting in a quenched fluorescence signal. Enzyme-driven hydrolysis of the substrate, by collagenases and gelatinases, results in the separation of the dye molecules and the generation of a fluorescence signal. The increase in fluorescence is proportional to the proteolytic activity. When incubated with DQ collagen, but not DQ gelatin, CD44-null FDMs had reduced fluorescence signal compared to WT FDMs, indicating that CD44-null fibroblasts had reduced collagenase (Fig. 4C) but not gelatinase activity (Fig. S6E).

CD44 deficiency increases fibrogenic response and reduces tensile strength of scar tissue

Excess accumulation of fibrillar collagen is a hallmark of scar tissue formation and aberrant wound healing [60–62], To determine if the increase in fibrillar collagen accumulation observed at wound closure at day 11 persists after wound closure, WT and CD44-null wounds were harvested 9 weeks (ie. day 63), post-wounding. CD44-null scars showed an increase in fibrillar collagen accumulation, using 2P-SHG (Fig. 5A), no significant difference in type I collagen accumulation, using IF (Fig. 5B), and reduced collagenase activity compared to WT scar tissue (Fig. 5C). WT and CD44-null scars showed no significant differences in HA or CD45^{+} leukocytes (Fig. S7A – C). Furthermore, CD44 deficiency had no significant impact on fibrillar collagen length, width, or angle analyzed

using CTfire (Fig. S7D – G). CD44-null scar tissue revealed an increase in FN accumulation and total mesenchymal fibroblasts (vimentin$^+$ area) but no significant changes in subsets of activated fibroblasts (FAP$^+$ or α-SMA$^+$ area) compared to WT (Fig. 5D, E, Fig. S7H, I). These results indicate that CD44-deficient scars had an overall increase in the fibroproliferative response.

Scar tissue has compromised biomechanics compared to normal skin. Due to alterations in amount and architecture of fibrillar collagen present, scars can potentially regain a maximum of 80% tensile strength compared to normal skin [2,3], To examine whether the increased fibrotic response we observed in scars in CD44-null mice impacted biomechanical properties of the scar tissue, the tensile strength of WT and CD44-null wounds were analyzed day 63 post-wounding. WT and CD44-null scars were extracted using a stamp to obtain samples of comparable size and shape. Samples were subjected to a ramp to failure test and tensile strength (Megapascal - MPa) was calculated using the slope (of the linear region) of a stress-strain curve. Using ramp to failure test, CD44-null scar tissue had reduced tensile strength compared to WT scars (Fig. 5F). Taken together, these data indicate that the increased accumulation of fibrillar collagen in CD44-null scars correlated to compromised tissue biomechanics.

Discussion

In summary, we show that loss of CD44 impacts inflammation, fibrogenesis and matrix remodeling during various stages of cutaneous wound healing (Fig. 6). Specifically, during early stages of wound healing, loss of CD44 enhanced the kinetics of leukocyte infiltration while delaying the accumulation and altering the spatial distribution of FAP$^+$ fibroblasts. The effect of FAP$^+$ fibroblasts was selective in that loss of CD44 had no impact on the kinetics or spatial distribution of total mesenchymal cells or α-SMA$^+$ myofibroblasts. Finally, loss of CD44 reduced collagen early – consistent with FAP$^+$ fibroblasts being a major source of collagen [48,52], However, by day 11 loss of CD44 was associated with an increased accumulation of collagen, due at least in part to a reduction in collagenolysis, which persisted in late scar tissue (day 63) and was associated with reduced tensile strength of scar tissue.

Increased HA accumulation has been reported to contribute to scarless healing in fetal wounds compared to adult wounds [63], Given the role of CD44 in mediating HA endocytosis [12,13], one posited mechanism by which HA contributes to scarless healing in fetal wounds is through its predominant receptor, CD44. As suggested by previous studies, here we have shown that HA accumulation begins at early stages of wound healing and is prevalent throughout the wound response; however, we found that genetic deletion of CD44 did not alter the total amounts of HA accumulation. This suggests that a compensatory mechanism may offset for CD44 deletion with regards to HA accumulation in our cutaneous wound healing model. In addition to CD44, HA can bind to other receptors such as receptor for HA-mediated motility (RHAMM) and intracellular adhesion molecule-1 (ICAM-1). These findings indicate that CD44 deletion is not sufficient to increase HA accumulation post-wounding, and further studies need to be conducted to understand the regulation of HA

synthesis, signaling via other receptors, and interaction with additional CD44 ligands such as fibronectin and collagen during cutaneous wound healing.

Fibroblasts are a heterogeneous population of cells that play a critical role in the dynamics of ECM composition and architecture [47,48], In an *in vitro* wound healing model, CD44 was required for directional migration of fibroblasts [22], Similarly, CD44-null fibroblasts isolated after acute lung injury showed reduced invasion into a fibrin gel and adhesion to provisional matrix components such as fibrin, fibrinogen, fibronectin, and HA [24], However, we found that in an *in vivo* cutaneous wound healing model, CD44-deficiency did not alter total fibroblast accumulation based on quantification of vimentin$^+$ area, in the granulation tissue. These data suggest that CD44 is either dispensable for fibroblast accumulation in this setting or that compensatory mechanisms such as upregulation of other adhesion molecules implicated in adhesion and migration, including integrins [33], may overcome the lack of CD44. Evaluation of integrin expression in WT and CD44-null wounds and loss of function experiments in future studies will help understand the cross-talk between CD44 and integrins in regulating fibroblast migration in response to cutaneous wound healing.

Traditionally, α-SMA was considered the primary marker for activated fibroblasts during cutaneous wound healing. Our data shows that similar to models of fibrosis and solid tumors, during cutaneous wound healing FAP and α-SMA identify distinct, and sometimes to varying degrees, overlapping cell populations [49–54], α-SMA, is the canonical marker for myofibroblasts with contractile properties [64], Using a mouse model with genetic deletion of α-SMA, multiple papers have reported that α-SMA facilitates but is not necessary for wound contraction and closure [65,66], These data also suggest that α-SMA is significant but not the only fibroblast protein involved in wound healing. Extrapolating from this hypothesized role in wound contraction, using IHC we found that α-SMA$^+$ cells are concentrated at the wound edge and close to the epidermis during early stages of wound healing, suggesting that α-SMA aides in the contraction of the wound edge. α-SMA$^+$ cells peaked at wound closure (day 11) and were dispersed throughout the granulation tissue, but were primarily concentrated near the epidermis. We found that WT and CD44-null mice had no significant differences in α-SMA$^+$ cells, which was consistent with comparable rates of wound closure observed.

Importantly, in WT wounds, we found that FAP$^+$ cells, but not α-SMA$^+$cells, account of the bulk of total fibroblasts in the granulation tissue during early phases of wound healing, when the ratio of FN to collagen is much higher in the granulation tissue. Furthermore, we found that during early phases of wound healing (day 5), FAP$^+$ cells are concentrated proximal to the hypodermis. The hypodermis lies between the dermis and underlying muscle and contains loose connective tissue and adipose tissue. Using an indentation test, the elastic modulus of human hypodermis is approximated to be 2 kPa [67], This is in line with recent data from our lab that showed selective differentiation of fibroblasts to a FAP^{hi} phenotype on soft (2 kPa) rather than stiff (20 kPa) FN-coated hydrogels [48] and evidence in the field highlighting the importance of the mechanical properties of provisional matrix on cellular migration and behavior [68], Additionally, we found that CD44 deficiency reduced the number of FAP$^+$ cells in the granulation tissue during early phases of wound healing. Taken

together, these data suggest that CD44 may play a critical role in the recruitment and/or generation of FAP^+ fibroblasts in response to tissue injury.

Gene expression profiling of FAP^{hi} fibroblasts revealed higher levels of various ECM components (including collagens) compared to α-SMA^{hi} fibroblasts [48], Similarly, depletion of FAP^+ cells has been shown to reduce the desmoplastic response in tumors [52]. Analogously, our data reveled that reduced FAP^+ fibroblasts in CD44-null wounds during early phases of wound healing correlated with reduced fibrillar collagen accumulation. These data suggest a potential role of FAP^+ cells in mediating the deposition of the early provisional matrix during cutaneous wound healing.

A potential mechanism for recruitment or activation of FAP^+ fibroblasts is the cross talk between inflammatory/immune cells and mesenchymal cells. One of the earliest events following tissue injury is activation of the innate immune response followed by monocytes, macrophages and lymphocytes [6,37]. Each cell type plays a vital role in the repair process; however, genetic studies have shown that no particular cell type is essential for overall healing [69]. There is evidence supporting the hypothesis that prolonged acute inflammation can delay early tissue restoration and fibrotic processes including keratinocyte proliferation, and recruitment of pro-fibrotic macrophages (M2 macrophages) [70,71]. We found that at day 5 post-wounding, CD44 deficiency increased the number of leukocytes and pro-inflammatory cytokines, including IL-4 and IL-1 *β*. This was accompanied by delayed recruitment of FAP^+ fibroblasts and fibrillar collagen accumulation. These data suggest that future studies need to be conducted to delineate if resolution of early inflammation or IL-4 and IL-1 β play an essential role in recruitment of FAP^+ fibroblasts and accumulation of fibrillar collagen during early phases of wound healing. By day 7 post-wounding, the increase in leukocyte accumulation found in CD44-null wounds did not correlate to alterations in cytokine levels. These data suggests that at day 7 post-wounding, either the increase in leukocytes is not sufficient to increase cytokine levels or that an increase in additional cell types, such as mesenchymal cells, offsets the increase in leukocyte. Further studies need to be conducted to delineate the cross-talk between fibroblasts and inflammatory cells in regulating cytokine levels during early phases of wound healing.

An interesting finding from our study was that CD44 deficiency increased fibrillar collagen accumulation in closed wounds, scar tissue, and in an *in vitro* model of fibroblast-derived matrices. Collagen has been a speculated CD44 ligand [18], Soluble CD44 (sCD44), generated after cleavage from extracellular membrane, can be integrated bind to ECM components including collagen [21], Immunoprecipitation studies have also demonstrated collagen XIV, a fibril associated collagen, can directly interact with CD44 [72]. Despite this evidence for collagen-CD44 interactions, few studies have investigated the role that CD44 plays in collagen accumulation or organization. In models of infarct healing and renal fibrosis, CD44-null mice had reduced total collagen accumulation, myofibroblast infiltration and impaired TGF-β signaling [29,73], On the other hand, in atherosclerosis CD44 deficiency had increased fibrous cap formation [32], In a bleomycin induced lung injury model, CD44-null mice showed no significant differences in pulmonary fibrosis [31]. Combined, these data indicate that the role of CD44 in collagen accumulation is tissue, injury and context dependent. A possible hypothesis for these paradoxical roles of CD44 in

collagen accumulation is the nearly ubiquitous expression of CD44 on various cell types present in response to injury. Therefore, depending on the milieu, CD44 can play contradictory roles. Keeping this in mind, in our current study we analyzed wounds during early inflammatory (day 5), late inflammatory (day 7), remodeling (day 11), and resolution (day 63) phases. During early and late inflammatory phases, we found that CD44-null mice had reduced fibrotic response, including reduced FAP^+ activated fibroblasts and fibrillar collagen accumulation. However, during remodeling and resolution phases we found that CD44-null mice had increased fibrillar collagen. This data supports the hypothesis that the role of CD44 in collagen accumulation is contextually regulated.

In order to elucidate the role of CD44 in collagen biosynthesis and turnover, day 11 wounds were biochemically analyzed. Collagen post-translational modifications include hydroxylation of proline and lysine residues, O-glycosylation of hydroxylysine residues, and intermolecular crosslinking. Post-translational modification of collagen is crucial for the stability of the triple-helical conformation of fibrillar collagen [74,75]. CD44-null wounds exhibited no differences in the level of hydroxylated proline residues or lysl oxidase at day 11 post-wounding or *in vitro* FDMs compared to WT controls. Collagen crosslinking and architecture have been identified as determinants of tensile strength in scar tissue [2,3,34,76]. In a normal skin, fibrillar collagen is present in a “basket weave” orientation, but in a scar tissue fibrillar collagen is present in greater amounts, and is accumulated in large bundles parallel to the length of the tissue. Due to the change in collage amounts and architecture, scar tissue is more susceptible to rupture/tear when stretched [34]. Consistent with these observations, we found that increased fibrillar collagen accumulation observed in CD44-null scar tissue was associated with concomitant reduction tensile strength. We also found that majority of collagen fibers were aligned parallel to the length of the tissue. However, we did not observe any differences between WT and CD44-null fibrillar collagen width, length and angle in scar tissue. These data suggest that in this setting, CD44 may not play a significant role in collagen post-translational modification or crosslinking, although further in-depth studies would need to be conducted to support these results. For example, analysis of WT and CD44-null wounds for collagen crosslinking products dehydro-dihydroxylysinonorleucine (DHLNL), dehydro-hydroxylysinonorleucine (HLNL), and dehydro histidinohydroxymerodesmosine (HHMD) will further help elucidate the role of CD44 in collagen crosslinking.

While our data did not show any differences in collagen crosslinking, we found that CD44-null wounds had reduced collagenase activity. These data support prior evidence implicating CD44 in cell surface MMP9 localization [14], MMP2 and MMP9 expression in tumor cells [77], and MMP activation in tumor cells [78]. Our results indicate that FDMs derived from CD44-null fibroblasts and CD44-null wounds have reduced collagenase activity and increased fibrillar collagen accumulation compared to WT controls. These results indicate that CD44 mediated collagen proteolysis regulates fibrillar collagen accumulation during cutaneous wound healing.

Prior studies have demonstrated the role of CD44 in various pathophysiological states including mouse models of cancer, atherosclerosis, pulmonary fibrosis and bacterial infections [21,25,30,32,41,42,78–80]. The impact of CD44 in these models can at least in

part be attributed to CD44-mediated signal transduction induced by HA engagement of the receptor and thereby regulating leukocyte trafficking, cell proliferation, actin-cytoskeletal remodeling, and vascular smooth muscle cell differentiation. However, CD44 has also been implicated in T-lymphocyte migration within tumors independent of the HA binding motif contained within the extracellular domain [81]. CD44 can also function as a docking platform for various matricellular proteins, proteases, and growth factors as well as molecular interactions with other cell surface molecules such as c-Met [17]. Herein, we demonstrate a novel role for CD44 in the fibro-inflammatory response to cutaneous injury. Our data indicate that in this context CD44 acts through regulating remodeling of the collagen-rich matrix and that CD44-dependent matrix remodeling contributes to resolution of the response to injury. In light of these new findings, it will be interesting to explore the mechanisms involved in the CD44-dependent collagen rich matrix remodeling and to assess the functional outcome of CD44-dependent matrix remodeling in other pathophysiological settings.

Material and Methods

Animals

WT BALB/c mice were purchased from Charles River Laboratory Inc. CD44-null mice [41] were backcrossed 12 generations onto a BALB/c background. Mice were used between 10 – 16 weeks of age. All mice were housed in University of Pennsylvania facilities, and all research was overseen by University Laboratory Animal Resources (ULAR). Experimental protocols were approved by the Institutional Animal Care and Use Committee and were in compliance with the Guideline for the Care and Use of Animals.

Generation of full-thickness excisional wounds

Mice were anesthetized using isoflurane (Henry Schein) and two equidistant 6-mm full thickness excisional wounds were generated using biopsy punches (Miltex) in the dorsal skin 4 mm below the shoulder blades. The wounds were covered using curad dressing (Medline) and tegaderm adhesive tape (Medline). Wound closure was determined by taking digital pictures every other day. Mice were sacrificed 5, 7, 11, or 63 days after wounding using CO_2.

Immunohistochemistry (IHC) and immunofluorescence (IF) analysis

Skin samples were collected, fixed in prefer (Anatech Ltd.), and paraffin-embedded. Skin samples were laterally bisected through the midline and 5-μm sections were mounted onto positively charged glass slides. Hematoxylin and eosin staining was conducted by the Penn Vet comparative pathology core. Masson's Trichrome Staining Kit (Sigma-Aldrich) was used to analyze total collagen accumulation as per manufacturers' instructions. Picrosirius Red staining was conducted using 0.1% Direct Red 80 (Sigma-Aldrich). For all other stains, tissue sections were wax-cleared, rehydrated then subjected to antigen retrieval (Table S1). For IHC, sections were blocked with avidin/biotin blocking kit (Vector Labs), 3% H_2O_2 (Sigma-Aldrich), and 10% goat serum prior to incubation with overnight primary antibody incubation in 10% goat serum in 1% BSA/PBS (Table S1). Sections were then incubated with secondary antibody in 1% BSA/PBS (Table S1), ABC Elite Reagent (Vector Labs), and

DAB (Dako). For IF, sections were blocked with 10% goat/donkey serum prior to primary antibody incubation (Table S2). Sections were then incubated with anti-FITC/TRITC (Table S2). To reduce tissue auto-fluorescence sections were treated with 0.1% Sudan black (in 70% ethanol) prior to counter staining with DAPI. For all staining, 10x (IHC) or 20x (IF) images were acquired using a Nikon Eclipse Ti-E inverted microscope. The motorized stage was utilized to obtain multichannel stitched-images of the entire skin section (including normal skin and granulation tissue). IHC and IF stain quantification was conducted using NIH Image J analysis software and NIS-elements analysis software.

Two-Photon Second-Harmonic Generation (2P-SHG)

Fibrillar collagen images were obtained using a Leica SP5 confocal/multiphoton (5-μm paraffin embedded sections day 7, 11, and decellularized FDMs) or a Leica SP8 confocal/multiphoton microscope (5-μm paraffin embedded sections day 5 and 63). 2P-SHG signal was obtained by tuning coherent chameleon Vision II Ti:Sapphire laser to 800 nm and an external non-descanned detector (HyD) configured to capture wavelengths <495 nm. Tissue autofluorescence signal was obtained by tuning two additional non-descanned detectors to 495 to 560 nm and 560 to 620 nm wavelengths. Fibrillar collagen images were obtained by subtracting autofluorescnce signal from the original SHG image. For wound healing samples, a motorized stage was utilized to obtain multichannel stitched-images of the entire skin section (including normal skin and granulation tissue). For decellularized matrices, 5 SHG images were acquired per matrix, and each experiment was conducted in triplicate.

Curvelet Transform Fiber Extraction Analysis (CT Fire Analysis)

Quantitative evaluation of collagen fibers were conducted as previously described [82]. A binary image was formed based on manually selected threshold parameters using the FIRE algorithm to detect fibers and eliminate potential background pixels. A preprocessed algorithm was then utilized to quantify fiber angle, length, width, and straightness.

In-situ Zymography

MMP activity was measured using in-situ zymography as previously described [83]. 5-μm paraffin embedded sections were wax-cleared and rehydrated. As per manufacturers instructions, skin sections were incubated with DQ Gelatin or DQ Collagen 1:200 (Thermofisher) in reaction buffer (50 mM Tris, 150 mM NaCI, 5 mM $CaCl_2$, 0.2 mM NaN_3) for 2 hours. Control sections were treated with reaction buffer alone (no DQ Gelatin or DQ Collagen). Sections were then treated with Sudan black, counterstained with DAPI and mounted with slowfade gold (Thermofisher). Using a motorized stage, 20x fluorescence images of the entire skin section were acquired using a Nikon Eclipse Ti-E inverted microscope.

Isolation of primary dermal fibroblasts

Primary dermal fibroblasts were isolated from naïve unwounded 10 – 16 weeks old WT and CD44-null BALB/c mice. Dorsal and ventral skin sections were finely minced and digested using 1 mg/ml collagenase type II (Worthington) and hyaluronidase (Sigma-Aldrich) in DMEM (Corning Inc.) at 37°C for 1.5 hours. Digestion was quenched using equal volume of

10% fetal calf serum (FCS) DMEM, strained through a 70 μm cell strainer (Corning Inc.), and pelleted by centrifugation at 1200 rpm for 5 minutes at 4°C. Cell pellets were washed with PBS (Corning Inc.) and resuspended in 10% FCS-DMEM containing 0.02 M HEPES, 1mM L-Glutamine, 10 units penicillin and 10 μg streptomycin, 0.05 mg gentamicin, and 0.25 μg amphothericin B and plated on tissue culture-treated plastic (polystyrene). Cells were maintained at 37 °C with 5% CO_2 in a humidified incubator. The following day, cell monolayers were thoroughly washed with PBS and supplemented with fresh media. Cells were maintained in 10% FCS DMEM on tissue culture-treated plastic for one passage. First passage fibroblasts were used for all experiments.

Fibroblast-Derived Matrices (FDMs)

FDMs were generated as previously described [58]. 5.0×10^5 first passage dermal fibroblasts were plated onto 0.2% cross-linked gelatin (Fisher Scientific) coated 35-mm plates. The next day, fibroblasts were supplemented with 75 μg/ml of ascorbic acid (Fisher Scientific), which was replenished every 48 hours for 8 days. Matrices were decellularized for matrix analysis using detergent treatment with 0.5% Triton X-100, 20 mM NH_4OH in PBS for 5 minutes at 37°C [84].

Calcein AM

Cell viability was analyzed using a calcein AM cell permanent dye as per manufacturer's instructions. On 8^{th} day of matrix production, FDMs were washed twice with PBS and then incubated with 1 μm calcein AM for 30 minutes at room temperature. Fluorescence excitation was measured at 485 nm. Data was represented as raw fluorescence units (RFU).

Quantitative Real-Time PCR

A 4 mm biopsy punch was used to extract wounds at closure (day 11 post-wounding). Samples were flash frozen using liquid nitrogen and crushed with a mortar and pestle on dry ice. RNA isolation was conducted using TriZol (Invitrogen) as per manufacturer's instructions. Gel electrophoresis was conducted to ensure RNA quality. 1 μg RNA was utilized for cDNA synthesis using TaqMan Reverse Transcription kit (Applied Biosystem). Transcript levels were quantified using StepOnePlus Real-Time PCR System (Applied Biosystems) and SYBR Green (Invitrogen). All samples were run in triplicate and averaged. mRNA levels for each gene of interest were normalized to Hprt. Primer Sequences: Hprt1-F, `5′-tgacactggtaaaacaatgca`; Hprt1-R, `5′-ggtccttttcaccagcaagct`; Mmp2-F, `5′-cccatgaagccttgtttacca`; Mmp2 -R, `5′-tggaagcggaacgggaact`; Mmp14-F, `5′-ccgaccgcgctctagga`; Mmp14-R, `5′- cgcgccgcctctctt`; Mmp8-F, `5′-aaaagggaagctcagtctgtatactc`; Mmp8-R, `5′- agagggctgcagagttagttacca`; Mmp9-F, `5′- tatttttgtgtggcgtctgagaa`; Mmp9-R, `5′- gaggtggtttagccggtgaa`; Lox-F, `5′-gggagtggcacagctgtca`; Lox-R, `5′- tcctctgtgtgttggcatcaag`.

Immunoblot

A 6 mm biopsy punch was used to extract wounds days 5 and 7 post-wounding. Samples were flash frozen using liquid nitrogen and crushed with a mortar and pestle on dry ice. Protein lysates were obtained using RIPA lysis buffer (Thermofisher) and were

supplemented with complete protease inhibitor tablets (Sigma-Aldrich), sodium orthovanadate, and sodium fluoride. Protein concentration was measured using a BCA protein assay kit (Thermofisher). 10 μg of protein was loaded onto a 4 – 12% Bis/Tris Mini Gel (Thermofisher), transferred onto PVDF membrane, and probed with antibodies to anti-MRC2 (Endo 180, abeam), β-Actin (Cell Signaling), followed by HRP-conjugated goat anti-rabbit secondary antibody (Sigma-Aldrich).

ELISA

Analysis of IL-4 (eBioscience), IL-1β (eBioscience), IL-10 (eBioscience), and TNF-α (eBioscience) in wound samples were conducted using above mentioned protein lysates as per manufacturer's instructions.

Flow Cytometry

Dorsal and ventral skin samples were extracted from 10 – 16 week old WT and CD44-null mice and digested using 10 ml of 1 mg/ml collagenase type II and hyaluronidase in DMEM for 2 hours at 37°C. Tissue lysates were then filtered through 70- and 40-μm cell strainer (Corning Inc.). For FDM experiments, cells depositing matrices were treated with 2 ml of 500 μg/ml of collagenase type I (Worthington) in DMEM for 30 minutes followed by 5 minutes trypsinization 37°C and filtration through a 70-μm cell strainer. The obtained single-cell suspension was stained for viability using aqua live/dead fixable cell stain kit (Molecular Probes). Extracellular stromal cell analysis was conducted using antibodies listed Supplemental Table 3. Prior to intracellular staining with anti-αSMA FITC 1:540 (Sigma Aldrich), cell suspension was fixed and permeabilized using cytofix/cytoperm fixation permeabilization kit (BD Bioscience). Unstained, LIVE/DEAD only, and single stains were used as controls. Single cells were gated on using forward and side scatter width and height event characteristics. The specificity of the FAP antibody was verified using FAP-null fibroblasts. Flow cytometric analyses were performed on a LSR-Fortessa using FACSDiva software (BD Bioscience) and data were analyzed using FlowJo (Tree Star).

Hydroxyproline Assay

Hydroxyproline assay was conducted as previously described [85]. 4 mm normal and wounded skin biopsies were weighed, cut and digested overnight at 110°C in 1 ml of 6N HCI. After neutralization with equal volume 6N NaOH, the pH was adjusted (6.0<pH<10.0). FDMs were treated with 100 μl 6N NaOH, collected using a cell scraper, and digested at 110°C for 20 minutes. Samples (100 μl) were mixed with 1 ml chloramine T solution for 20 minutes at room temperature, followed by 1 ml erlich's solution (Sigma Aldrich) and incubated at 65°C for 15 minutes. 200 μl aliquots were transferred to 96-well plates, and absorbance was measured at 570 nm. Collagen content was calculated by comparison with a standard curve generated with cis-4 hydroxy-L-proline (0.01–110 μg/ ml; Sigma-Aldrich), using the conversion factor of 1 μg hydroxyproline, corresponding to 6.94 μg collagen. Total collagen was expressed as μg collagen normalized to mg of tissue weight or raw fluorescence unit corresponding to calcein AM signal.

HA Purification and ELISA

4 mm biopsy punches were conducted to obtain normal skin samples. HA purification was conducted by digesting skin samples in 10 mg/ml proteinase K in ammonium acetate at 60°C for 4 hours. 4 volumes of pre-chilled 200 proof ethanol was added and samples were incubated at −20°C overnight. Samples were then pelleted by centrifugation at 14,000 g for 10 minutes at room temperature followed by 4 volumes of pre-chilled 75% ethanol and re-pelleted by centrifugation at 14,000 g for 10 minutes. Pellets were air-dried and resuspended in 100 μl 100 mM ammonium acetate. A second ethanol precipitation was conducted by repeating aforementioned protocol and samples were resuspended in 20 ul of 100 mM ammonium acetate. Total amount of HA was quantified using Hyaluronan DuoSet ELISA Kit (R&D) as per manufacturer's instructions.

Tensile Strength Analysis

Wound samples were extracted using a standardized method via the use of a dog-bone punch resulting in a gauge length of 10mm and width of 2.5mm at the smallest cross-section. The cross-sectional area of the samples was measured at 5 locations via a custom laser-based measuring device [86]. The final area was determined as the average of these five readings. Sample termini were sandwiched between sandpaper (grit = 400) using cyanoacrylate glue. The dog-bone skin samples were then placed in metal clamps and tested in an Instron 5542 materials testing machine (Instron Inc.). The mechanical testing protocol consisted of a preload to 0.25N followed by a 60 second hold to collect gauge length images. This was followed by a ramp to failure at a ramp rate of 0.24mm/sec till failure of the sample occurred. Parameters collected were: maximum load (N), maximum strain (mm/mm), stiffness (N/mm, slope of the linear region from the load-displacement curve), maximum stress (N/mm^2, maximum load divided by the cross-sectional area), and Young's modulus (N/mm^2, slope of the linear region from the stress-strain curve).

Statistical Analysis

All results are expressed as mean ± SEM. Statistical analysis was performed using 2-tailed student's t test (GraphPad Prism 7.0). Asterisks denote statistical significance: **** $p < 0.0001$, *** $p < 0.001$, ** $p < 0.01$, * $p < 0.05$.

Supplementary Material

Refer to Web version on PubMed Central for supplementary material.

Acknowledgements

We thank Dr. Susan Volk for helpful discussions that facilitated the design of experiments and conception of the manuscript. We thank the PCMD Biomechanics Core for conducting the tensile strength analysis and the histology facility at the Ryan Hospital of the School of Veterinary Medicine at the University of Pennsylvania. The authors declare no competing financial interests.

Funding

This work was supported by a grant from the NIH P30 AR069619 (PCMD Biomechanics Core).

Abbreviations:

HA	Hyaluronic Acid
ECM	Extracellular Matrix
MMP-9	Matrix Metalloproteinase-9
VEGF	Vascular Endothelial Growth Factor
EGF	Epidermal Growth Factor
TGF-β	Transforming Growth Factor-Beta
VSMC	Vascular Smooth Muscle Cells
2P-SHG	Two-photon Second Harmonic Generation
FN	Fibronectin
FAP	Fibroblast Activation Protein
αSMA	Alpha-Smooth Muscle Actin
RHAMM	Receptor for HA-Mediated Motility
ICAM-1	Intracellular Adhesion Molecule-1
LOX	Lysyl Oxidase
sCD44	soluble CD44
FDMs	Fibroblast Derived Matrices
IHC	Immunohistochemistry
IF	Immunofluorescence
DHLNL	dehydro-dihydroxylysinonorleucine
HLNL	dehydro-hydroxylysinonorleucine
HHMD	dehydro-histidinohydroxymerodesmosine

References

[1]. Corr DT, Hart DA, Biomechanics of Scar Tissue and Uninjured Skin, Adv. Wound Care. 2 (2013) 37–3. doi:10.1089/wound.2011.0321.

[2]. Brenda E, Marques a., Saldiva PHN, Davini MC, Pereira MD, Minami E, Ferreira MC, Analysis of the collagen content and tensile strength of the aponeurotic scar - an experimental study in pigs, Eur. J. Plast. Surg 22 (1999) 28–35. doi:10.1007/s002380050140.

[3]. Eleswarapu SV, Responte DJ, Athanasiou KA, Tensile properties, collagen content, and crosslinks in connective tissues of the immature knee joint, PLoS One. 6 (2011) 1–7. doi:10.1371/journal.pone.0026178.

[4]. Singer AJ, Clark RAF, Cutaneous Wound Healing, N. Engl. J. Med 341 (1999) 738–746. [PubMed: 10471461]

[5]. Flanagan M, The physiology of wound healing, J. Wound Care. 9 (2000) 299–300. [PubMed: 11933346]

[6]. Gurtner GC, Werner S, Barrandon Y, Longaker MT, Wound repair and regeneration, Nature. 453 (2008) 314–321. doi:10.1038/nature07039. [PubMed: 18480812]

[7]. Baker R, Urso-Baiarda F, Linge C, Grobbelaar A, Cutaneous scarring: A clinical review, Dermatol. Res. Pract. 2009 (2009). doi: 10.1155/2009/625376.

[8]. Bayat a, a McGrouther D, Ferguson MWJ, Skin scarring., BMJ. 326 (2003) 88–92. doi: 10.1136/bmj.326.7380.88. [PubMed: 12521975]

[9]. Volk SW, Wang Y, Mauldin EA, Liechty KW, Adams SL, Diminished type III collagen promotes myofibroblast differentiation and increases scar deposition in cutaneous wound healing, Cells Tissues Organs. 194 (2011) 25–37. doi: 10.1159/000322399. [PubMed: 21252470]

[10]. Mast BA, Haynes JH, Krummel TA, Diegelmann RF, Cohen IK, In Vivo Degradation of Fetal Wound Hyaluronic Acid Results in Increased Fibroplasia, Collagen Deposition, and Neovascularization, Plast. Reconstr. Surg 89 (1992) 503–509. [PubMed: 1371361]

[11]. Dillion PW, Keefer K, Blackburn JH, Houghton PE, Krummel TM, The Extracellular Matrix of Fetal Wounds: Hyaluronic Acid Controls Lymphocyte Adhesion, J. Surg. Res 57 (1994) 170–173. [PubMed: 8041133]

[12]. Jiang H, Peterson RS, Wang W, Bartnik E, Knudson CB, Knudson W, A requirement for the CD44 cytoplasmic domain for hyaluronan binding, pericellular matrix assembly, and receptor-mediated endocytosis in COS-7 cells, J. Biol.Chem 277 (2002) 10531–10538. doi:10.1074/jbc.M108654200. [PubMed: 11792695]

[13]. Rahmanian M, Heldin P, Testicular Hyaluronidase Induces Tubular Structures of Endothelial Cells Grown in Three Dimensional Collagen Gel through a CD44- mediated Mechanism, Int. J. Cancer. 97 (2002) 601–607. [PubMed: 11807784]

[14]. Yu Q, Stamenkovic I, Cell surface-localized matrix mealloproteinase-9 proteolytically activates TGF-beta and promotes tumor invasion and angiogenesis, Genes Dev. 14 (2000) 163–176. doi: 10.1101/gad.14.2.163. [PubMed: 10652271]

[15]. Volz Y, Koschut D, Matzke-Ogi A, Dietz MS, Karathanasis C, Richert L, Wagner MG, Mely Y, Heilemann M, Niemann HH, Orian-Rousseau V, Direct binding of hepatocyte growth factor and vascular endothelial growth factor to CD44v6, Biosci. Rep 35 (2015) e00236–e00236. doi: 10.1042/BSR20150093. [PubMed: 26181364]

[16]. Jalkanen S, Jalkanen M, Lymphocyte CD44 binds the COOH-terminal heparin binding domain of fibronectin, J. Cell Biol. 116 (1992) 817–825. doi:10.1083/jcb.116.3.817. [PubMed: 1730778]

[17]. Puré E, Assoian RK, Rheostatic signaling by CD44 and hyaluronan, Cell Signal. 21 (2009) 651–655. doi:10.1016/j.cellsig.2009.01.024.Rheostatic. [PubMed: 19174187]

[18]. Naor D, Sionov RV, Ish-Shalom D, CD44: Structure, Function and Association with the Malignant Process, Adv. Cancer Res 71 (1997) 241–319. [PubMed: 9111868]

[19]. Faassen AE, Schrager JA, Klein DJ, Oegema TR, Couchman JR, McCarthy JB, A cell surface chondroitin sulfate proteoglycan, immunologically related to CD44, is involved in type I collagen - mediated melanoma cell motility and invasion, J. Cell Biol 116 (1992) 521–531. [PubMed: 1730766]

[20]. Midgley AC, Rogers M, Hallett MB, Clayton A, Bowen T, Phillips AO, Steadman R, Transforming growth factor-Beta 1 (TGF-BI)-stimulated fibroblast to myofibroblast differentiation is mediated by hyaluronan (HA)-facilitated epidermal growth factor receptor (EGFR) and CD44 co-localization in lipid rafts, J. Biol. Chem 288 (2013) 14824–14838. doi: 10.1074/jbc.M113.451336. [PubMed: 23589287]

[21]. Cichy J, Bals R, Potempa J, Mani A, Pure E, Proteinase-mediated release of epithelial cell-associated CD44: Extracellular CD44 complexes with components of cellular matrices, J. Biol. Chem 277 (2002) 44440–44447. doi:10.1074/jbc.M207437200. [PubMed: 12226094]

[22]. Acharya PS, Majumdar S, Jacob M, Hayden J, Mrass P, Weninger W, Assoian RK, Pure E, Fibroblast migration is mediated by CD44-dependent TGF activation, J. Cell Sci 121 (2008) 1393–1402. doi:10.1242/jcs.021683. [PubMed: 18397995]

[23]. Razinia Z, Castagnino P, Xu T, Vázquez-Salgado A, Puré E, Assoian RK, Stiffness-dependent motility and proliferation uncoupled by deletion of CD44, Sci. Rep 7 (2017) 1–10. doi:10.1038/s41598-017-16486-z. [PubMed: 28127051]

[24]. Svee K, White J, Vaillant P, Jessurun J, Roongta U, Krumwiede M, Johnson D, Henke C, Acute lung injury fibroblast migration and invasion of a fibrin matrix is mediated by CD44, J. Clin. Invest 98 (1996) 1713–1727.doi:10.1172/JC1118970. [PubMed: 8878421]

[25]. Cuff CA, Kothapalli D, Azonobi I, Chun S, Zhang Y, Belkin R, Yeh C, Secreto A, Assoian RK, Rader DJ, Puré E, The adhesion receptor CD44 promotes atherosclerosis by mediating inflammatory cell recruitment and vascular cell activation, J. Clin. Invest 108 (2001) 1031–1040. doi:10.1172/JCI200112455. [PubMed: 11581304]

[26]. Jain M, He Q, Sen Lee W, Kashiki S, Foster LC, Tsai JC, Lee ME, Haber E, Role of CD44 in the reaction of vascular smooth muscle cells to arterial wall injury, J. Clin. Invest 97 (1996) 596–603. doi: 10.1172/JC1118455. [PubMed: 8609213]

[27]. Zhao G, Shaik RS, Zhao H, Beagle J, Kuo S, Hales CA, Low molecular weight (LMW) heparin inhibits injury-induced femoral artery remodeling in mouse via upregulating CD44 expression, J. Vase. Surg 53 (2011) 1359–1367.e3.doi: 10.1016/j.jvs.2010.11.048.

[28]. Moon C, Heo S, Sim KB, Shin T, Upregulation of CD44 expression in the spinal cords of rats with clip compression injury, Neurosci. Lett 367 (2004) 133–136. doi: 10.1016/j.neulet.2004.05.101. [PubMed: 15308314]

[29]. Huebener P, Abou-Khamis T, Zymek P, Bujak M, Ying X, Chatila K, Haudek S, Thakker G, Frangogiannis NG, CD44 Is Critically Involved in Infarct Healing by Regulating the Inflammatory and Fibrotic Response, J. Immunol 180 (2008) 2625–2633. doi: 10.4049/jimmunol.180.4.2625. [PubMed: 18250474]

[30]. Vandivier B, Jiang D, Liang CJ, Teder P, Vandivier RW, Jiang D, Resolution of Lung Inflammation by CD44, Science (80-.). 296 (2002) 155–159. doi: 10.1126/science.1069659.

[31]. Li Y, Jiang D, Liang J, Meltzer EB, Gray A, Miura R, Wogensen L, Yamaguchi Y, Noble PW, Severe lung fibrosis requires an invasive fibroblast phenotype regulated by hyaluronan and CD44, J. Exp. Med 208 (2011) 1459–1471. doi: 10.1084/jem.20102510. [PubMed: 21708929]

[32]. Zhao L, Lee E, Zukas AM, Middleton MK, Kinder M, Acharya PS, Hall JA, Rader DJ, Pure E, CD44 expressed on both bone marrow-derived and non-bone marrow-derived cells promotes atherogenesis in ApoE-deficient mice, Arterioscler. Thromb. Vase. Biol 28 (2008) 1283–1289. doi:10.1161/ATVBAHA.108.165753.

[33]. Greiling D, Clark RA, Fibronectin provides a conduit for fibroblast transmigration from collagenous stroma into fibrin clot provisional matrix, J. Cell Sci 110 (1997) 861 LP–870.http://jcs.biologists.Org/content/110/7/861.abstract. [PubMed: 9133673]

[34]. Xue M, Jackson CJ, Extracellular Matrix Reorganization During Wound Healing and Its Impact on Abnormal Scarring, Adv. Wound Care. 4 (2015) 119–136. doi:10.1089/wound.2013.0485.

[35]. Fronza M, Caetano GF, Leite MN, Bitencourt CS, Paula-Silva FWG, Andrade TAM, Frade MAC, Merfort I, Faccioli LH, Hyaluronidase modulates inflammatory response and accelerates the cutaneous wound healing, PLoS One. 9 (2014) 1–12. doi: 10.1371/journal.pone.0112297.

[36]. Dunn L, Prosser HCG, Tan JTM, Vanags LZ, Ng MKC, Bursill CA, Murine Model of Wound Healing, J. Vis. Exp (2013) 1–6. doi:10.3791/50265.

[37]. Eming SA, Krieg T, Davidson JM, Inflammation in wound repair: Molecular and cellular mechanisms, J. Invest. Dermatol. 127 (2007) 514–525.doi: 10.1038/sj.jid.5700701. [PubMed: 17299434]

[38]. Ogawa R, Keloid and hypertrophic scars are the result of chronic inflammation in the reticular dermis, Int. J. Mol. Sci. 18 (2017). doi: 10.3390/ijms18030606.

[39]. Mack M, Inflammation and fibrosis, Matrix Biol. (2017). doi:10.1016/j.matbio.2017.11.010.

[40]. Maiti A, Maki G, Johnson P, TNF-alpha induction of CD44-mediated leukocyte adhesion by sulfation, Science (80-.). 282 (1998) 941–943. doi: 10.1126/science.282.5390.941. [PubMed: 9794764]

[41]. Schmits R, Filmus J, Gerwin N, Senaldi G, Kiefer F, Kundig T, Wakeham A, Shahinian A, Catzavelos C, Rak J, Furlonger C, Zakarian A, Simard JJL, Ohashi PS, Paige CJ, Gutierrez-Ramos JC, Mak TW, CD44 regulates hematopoietic progenitor distribution, granuloma

formation, and tumorigenicity., Blood. 90 (1997) 2217–33. http://www.bloodjournal.Org/content/90/6/2217.abstract. [PubMed: 9310473]

[42]. Wang Q, Teder P, Judd NP, Noble PW, Doerschuk CM, CD44 deficiency leads to enhanced neutrophil migration and lung injury in Escherichia coli pneumonia in mice, Am. J. Pathol 161 (2002) 2219–2228. doi:10.1016/S0002-9440(10)64498-7. [PubMed: 12466136]

[43]. Barrientos S, Stojadinovic O, Golinko MS, Brem H, Tomic-Canic M, Growth factors and cytokines in wound healing, Wound Repair Regen. 16 (2008) 585–601. doi: 10.1111/j.1524-475X.2008.00410.x. [PubMed: 19128254]

[44]. Coussens LM, Werb Z, Inflammation and cancer, Nature. 420 (2002) 860–867. doi: 10.1038/nature01322. Inflammation. [PubMed: 12490959]

[45]. Elliott CG, Forbes TL, Leask A, Hamilton DW, Inflammatory microenvironment and tumor necrosis factor alpha as modulators of periostin and CCN2 expression in human non-healing skin wounds and dermal fibroblasts, Matrix Biol. 43 (2015) 71–84. doi:10.1016/j.matbio.2015.03.003. [PubMed: 25779637]

[46]. Ono M, Masaki A, Maeda A, Kilts TM, Hara ES, Komori T, Pham H, Kuboki T, Young MF, CCN4/WISP1 controls cutaneous wound healing by modulating proliferation, migration and ECM expression in dermal fibroblasts via α5β1 and TNFα, Matrix Biol. (2018) 1–14. doi: 10.1016/j.matbio.2018.01.004.

[47]. Sorrell JM, Caplan AI, Fibroblasts-A Diverse Population at the Center of It All, Int. Rev. Cell Mol. Biol 276 (2009) 161–214. doi:10.1016/S1937-6448(09)76004-6. [PubMed: 19584013]

[48]. Avery D, Govindaraju P, Jacob M, Todd L, Monslow J, Puré E, Extracellular matrix directs phenotypic heterogeneity of activated fibroblasts, Matrix Biol. (2017). doi:10.1016/j.matbio.2017.12.003.

[49]. Acharya PS, Zukas A, Chandan V, Katzenstein ALA, Puré E, Fibroblast activation protein: A serine protease expressed at the remodeling interface in idiopathic pulmonary fibrosis, Hum. Pathol. 37 (2006) 352–360. doi:10.1016/j.humpath.2005.11.020. [PubMed: 16613331]

[50]. Levy MT, McCaughan GW, Abbott CA, Park JE, Cunningham AM, Muller E, Rettig WJ, Gorrell MD, Fibroblast activation protein: A cell surface dipeptidyl peptidase and gelatinase expressed by stellate cells at the tissue remodelling interface in human cirrhosis, Hepatology. 29 (1999) 1768–1778. doi: 10.1002/hep.510290631. [PubMed: 10347120]

[51]. Tillmanns J, Hoffmann D, Habbaba Y, Schmitto JD, Sedding D, Fraccarollo D, Galuppo P, Bauersachs J, Fibroblast activation protein alpha expression identifies activated fibroblasts after myocardial infarction, J. Mol. Cell. Cardiol 87 (2015) 194–203. doi: 10.1016/j.yjmcc.2015.08.016. [PubMed: 26319660]

[52]. Lo A, Wang LCS, Scholler J, Monslow J, Avery D, Newick K, O'Brien S, Evans RA, Bajor DJ, Clendenin C, Durham AC, Buza EL, Vonderheide RH, June CH, Albelda SM, Pure E, Tumor-promoting desmoplasia is disrupted by depleting FAP-expressing stromal cells, Cancer Res. 75 (2015) 2800–2810. doi: 10.1158/0008-5472.CAN-14-3041. [PubMed: 25979873]

[53]. Öhlund D, Handly-Santana A, Biffi G, Elyada E, Almeida AS, Ponz-Sarvise M, Corbo V, Oni TE, Hearn SA, Lee EJ, Chio IIC, Hwang C.-l., Tiriac H, Baker LA, Engle DD, Feig C, Kultti A, Egeblad M, Fearon DT, Crawford JM, Clevers H, Park Y, Tuveson DA, Distinct populations of inflammatory fibroblasts and myofibroblasts in pancreatic cancer, J. Exp. Med (2017) 579–596. doi: 10.1084/jem.20162024. [PubMed: 28232471]

[54]. Tchou J, Zhang PJ, Bi Y, Satja C, Marjumdar R, TL S, Chen H, Mies C, June CH, Conejo-Garcia J, Pure E, Fibroblast Activation Protein Expression by Stromal Cells and Tumor-Associated Macrophages in Human Breast Cancer, Hum. Pathol 44 (2013) 2549–2557. doi:10.1016/j.jneb.2009.11.007.lmpact. [PubMed: 24074532]

[55]. Prockop DJ, Kivirikko KI, Tuderman L, Guzman Norberto A, The Biosynthesis of Collagen and Its Disorders, N. Engl. J. Med 301 (1979) 77–85. doi: 10.1056/NEJM197107222850421. [PubMed: 36559]

[56]. Prockop DJ, Kivirikko K.l., Tuderman L, Guzman Norberto A, The Biosynthesis of Collagen and Its Disorders, N. Engl. J. Med 301 (1979) 13–23. doi: 10.1056/NEJM197107222850421. [PubMed: 449904]

[57]. McKleroy W, Lee T-H, Atabai K, Always cleave up your mess: targeting collagen degradation to treat tissue fibrosis, AJP Lung Cell. Mol. Physiol 304 (2013) L709–L721. doi:10.1152/ajplung.00418.2012.

[58]. Beacham D, Amatangelo M, Cukierman E, Preparation of Extracellular Matrices Produced by Cultured and Primary Fibroblasts, Curr. Protoc. Cell Biol 33 (2007). doi: 10.1002/0471143030.cb1009s33.

[59]. Schwarz R.l., Kleinman P, Owens N, Ascorbate Can Act as an Inducer of the Collagen Pathway Because Most Steps Are Tightly Coupled, Ann. N. Y. Acad.Sci 498 (1987) 172–185. doi: 10.1111/j.1749-6632.1987.tb23760.x. [PubMed: 3475997]

[60]. Wulandari E, Jusman SWA, Moenadjat Y, Jusuf AA, Sadikin M, Expressions of collagen I and III in hypoxic keloid tissue, Kobe J. Med. Sci 62 (2016) 58–69.

[61]. Takeo M, Lee W, Ito M, Wound healing and skin regeneration, Cold Spring Harb. Perspect. Med 5 (2015) 1–12. doi:10.1101/cshperspect.a023267.

[62]. Andrews JP, Marttala J, Macarak E, Rosenbloom J, Uitto J, Keloids: The paradigm of skin fibrosis—Pathomechanisms and treatment, Matrix Biol. 51 (2016) 37–46. doi:10.1016/j.matbio.2016.01.013.Keloids. [PubMed: 26844756]

[63]. Balaji S, Wang X, King A, Le LD, Bhattacharya SS, Moles CM, Butte MJ, De JesusPerez VA, Liechty KW, Wight TN, Crombleholme TM, Bollyky PL, Keswani SG, lnterleukin-10-mediated regenerative postnatal tissue repair is dependent on regulation of hyaluronan metabolism via fibroblast-specific STAT3 signaling, FASEB J. 31 (2017) 868–881. doi:10.1096/fj.201600856R. [PubMed: 27903619]

[64]. Hinz A, Celetta G, Tomasek JJ, Gabbiani G, Chaponnier C, Alpha-Smooth Muscle Actin Expression Upregulates Fibroblast Contractile Activity, Mol. Biol.Cell 12 (2001) 2730–2741. doi:10.1091/mbc.12.9.2730. [PubMed: 11553712]

[65]. Tomasek JJ, Haaksma CJ, Schwartz RJ, Howard EW, Whole animal knockout of smooth muscle alpha-actin does not alter excisional wound healing or the fibroblast-to-myofibroblast transition, 21 (2013) 166–176. doi:10.1111/wrr.12001. Whole.

[66]. Ibrahim M, Mohamed L Chen, Bond JE, Medina MA, Ren L, Kokosis G, Selim AM, Levinson H, Myofibroblasts contribute to but are not necessary for wound contraction, 95 (2015) 1429–1438. doi: 10.1126/science.1249098.Sleep.

[67]. Pailler-Mattei A, Bee S, Zahouani H, In vivo measurements of the elastic mechanical properties of human skin by indentation tests, Med. Eng. Phys 30 (2008) 599–606. doi:10.1016/j.medengphy.2007.06.011. [PubMed: 17869160]

[68]. Chester A, Brown AC, The role of biophysical properties of provisional matrix proteins in wound repair, Matrix Biol. 60-61 (2017) 124–140. doi:10.1016/j.matbio.2016.08.004. [PubMed: 27534610]

[69]. Martin P, Leibovich SJ, Inflammatory cells during wound repair: The good, the bad and the ugly, Trends Cell Biol. 15 (2005) 599–607. doi:10.1016/j.tcb.2005.09.002. [PubMed: 16202600]

[70]. Koh TJ, DiPietro LA, Inflammation and wound healing: The role of the macrophage, Expert Rev Mol Med. 16 (2013) 1–14. doi: 10.1017/S1462399411001943.Inflammation.

[71]. Landén NX, Li D, Ståhle M, Transition from inflammation to proliferation: a critical step during wound healing, Cell. Mol. Life Sci 73 (2016) 3861–3885. doi: 10.1007/s00018-016-2268-0. [PubMed: 27180275]

[72]. Ehnis T, Dieterich W, Bauer M, Von Lampe B, Schuppan D, A chondroitin/dermatan sulfate form of CD44 is a receptor for collagen XIV (Undulin), Exp. Cell Res 229 (1996) 388–397. doi: 10.1006/excr.1996.0384. [PubMed: 8986622]

[73]. Rouschop KMA, Sewnath ME, Claessen N, Roelofs JJTH, Hoedemaeker I, Van Der Neut R, Aten J, Pals ST, Weening JJ, Florquin S, CD44 Deficiency Increases Tubular Damage but Reduces Renal Fibrosis in Obstructive Nephropathy, J. Am. Soc. Nephrol 15 (2004) 674–686. doi: 10.1097/01.ASN.0000115703.30835.96. [PubMed: 14978169]

[74]. Chopra RK, Ananthanarayanan VS, Conformational implications of enzymatic proline hydroxylation in collagen., Proc. Natl. Acad. Sci. U. S. A. 79 (1982) 7180–4. doi: 10.1073/pnas.79.23.7180. [PubMed: 6296823]

[75]. Terajima M, Perdivara I, Sricholpech M, Deguchi Y, Pleshko N, Tomer KB, Yamauchi M, Glycosylation and cross-linking in bone type I collagen, J. Biol. Chem 289 (2014) 22636–22647. doi:10.1074/jbc.M113.528513. [PubMed: 24958722]

[76]. Depalle B, Qin Z, Shefelbine SJ, Buehler MJ, Influence of cross-link structure, density and mechanical properties in the mesoscale deformation mechanisms of collagen fibrils, J. Mech. Behav. Biomed. Mater. 52 (2015) 1–13.doi: 10.1016/j.jmbbm.2014.07.008. [PubMed: 25153614]

[77]. Chang G, Wang J, Zhang H, Zhang Y, Wang C, Xu H, Zhang H, Lin Y, Ma L, Li Q, Pang T, CD44 targets Na + /H + exchanger 1 to mediate MDA-MB-231 cells' metastasis via the regulation of ERK1/2, Br. J. Cancer. 110 (2014) 916–927. doi: 10.1038/bjc.2013.809. [PubMed: 24434427]

[78]. Desai B, Rogers MJ, Chellaiah MA, Mechanisms of osteopontin and CD44 as metastatic principles in prostate cancer cells, Mol. Cancer. 6 (2007) 1–16.doi: 10.1186/1476-4598-6-18. [PubMed: 17199893]

[79]. Nikitovic D, Kouvidi K, Karamanos NK, Tzanakakis GN, The roles of hyaluronan/RHAMM/CD44 and their respective interactions along the insidious pathways of fibrosarcoma progression, Biomed Res. Int 2013 (2013) 1–12. doi: 10.1155/2013/929531.

[80]. Sague SL, Tato C, Puré E, a Hunter C, The regulation and activation of CD44 by natural killer (NK) cells and its role in the production of IFN-gamma., J. Interferon Cytokine Res 24 (2004) 301–309. doi: 10.1089/107999004323065093. [PubMed: 15153314]

[81]. Mrass P, Kinjyo I, Ng LG, Reiner SL, Puré E, Weninger W, Successful interstitial navigation by killer T cells enables efficient anti-tumor immunity, 29 (2008) 971–985.doi:10.1016/j.immuni.2008.10.015.Successful.

[82]. Bredfeldt JS, Liu Y, Pehlke CA, Conklin MW, Szulczewski JM, Inman DR, Keely PJ, Nowak RD, Mackie TR, Eliceiri KW, Computational segmentation of collagen fibers from second-harmonic generation images of breast cancer, J. Biomed. Opt 19 (2014) 016007. doi: 10.1117/1.JBO.19.1.016007.

[83]. George SJ, Johnson JL, Matrix Metalloproteinase Protocols, 622 (2010) 271–277. doi: 10.1007/978-1-60327-299-5.

[84]. Lee HO, Mullins SR, Franco-Barraza J, Valianou M, Cukierman E, Cheng JD, FAP-overexpressing fibroblasts produce an extracellular matrix that enhances invasive velocity and directionality of pancreatic cancer cells, BMC Cancer. 11 (2011) 1–13. doi: 10.1186/1471-2407-11-245. [PubMed: 21194487]

[85]. Santos A, Jung J, Aziz N, Kissil J, Targeting fibroblast activation protein inhibits tumor stromagenesis and growth in mice, J. Clin. Invest 119 (2009) 3613–3625. doi: 10.1172/JCI38988DS1. [PubMed: 19920354]

[86]. Favata M, Beredijklian PK, Zgonis MH, Beason DP, Crombleholme TM, Jawad AF, Soslowskly LJ, Regenerative Properties of Fetal Sheep Tendon Are Not Adversely Affected by Transplantation into an Adult Environment, J. Orthop. Res 24 (2006) 2124–2132. doi: 10.1002/jor. [PubMed: 16944473]

Highlights

- CD44 deletion increases the kinetics of leukocyte infiltration while delaying the accumulation of FAP^+ fibroblasts and fibrillar collagen during early phases of wound healing.
- Spatial and temporal distribution of FAP^+, but not total mesenchymal cells or α-SMA^+ fibroblasts, is CD44 dependent.
- CD44-dependent collagenolysis regulates fibrillar collagen accumulation during the tissue-remodeling phase of wound healing and *in vitro*.
- CD44 deletion increases the fibrogenic response and reduces the tensile strength of scar tissue.

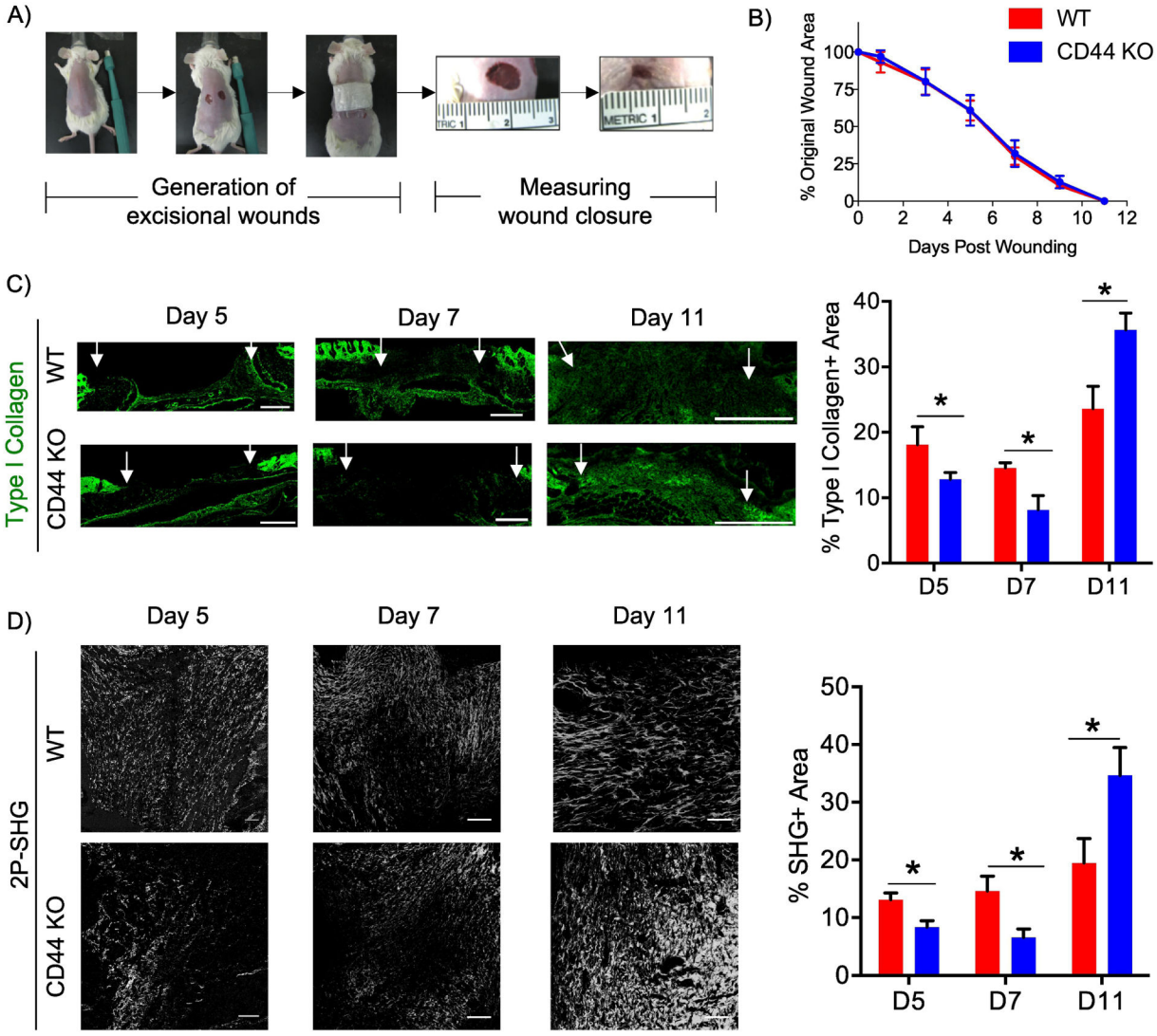

Figure 1. CD44 deficiency alters the kinetics of fibrillar collagen accumulation during cutaneous wound healing.

A) Representative images illustrating the generation of two 6 mm excisional biopsy punches on the dorsal side of WT and CD44 KO BALB/c mice. B) Quantitative measurement of wound area on days 1, 3, 5, 7, 9 and 11 post-wounding was conducted using the formula $A = \Pi r^2$. C) Representative 20x images of type I collagen staining of wounds extracted 5, 7, and 11 post-wounding (left), n=6-7 per group. White arrows indicate wound edges. Quantification of type I collagen staining normalized to total area of granulation tissue (right). Scale bars = 500μm D) Representative 20x images of two-photon second harmonic generation (2P-SHG) images to visualize fibrillar collagen accumulation of wounds extracted 5, 7, and 11 days post-wounding (left), n = 6-7 per group. Quantification of SHG signal (right). Scale bars = 200μm. Bar graphs depict mean ± SEM. * $p < 0.05$

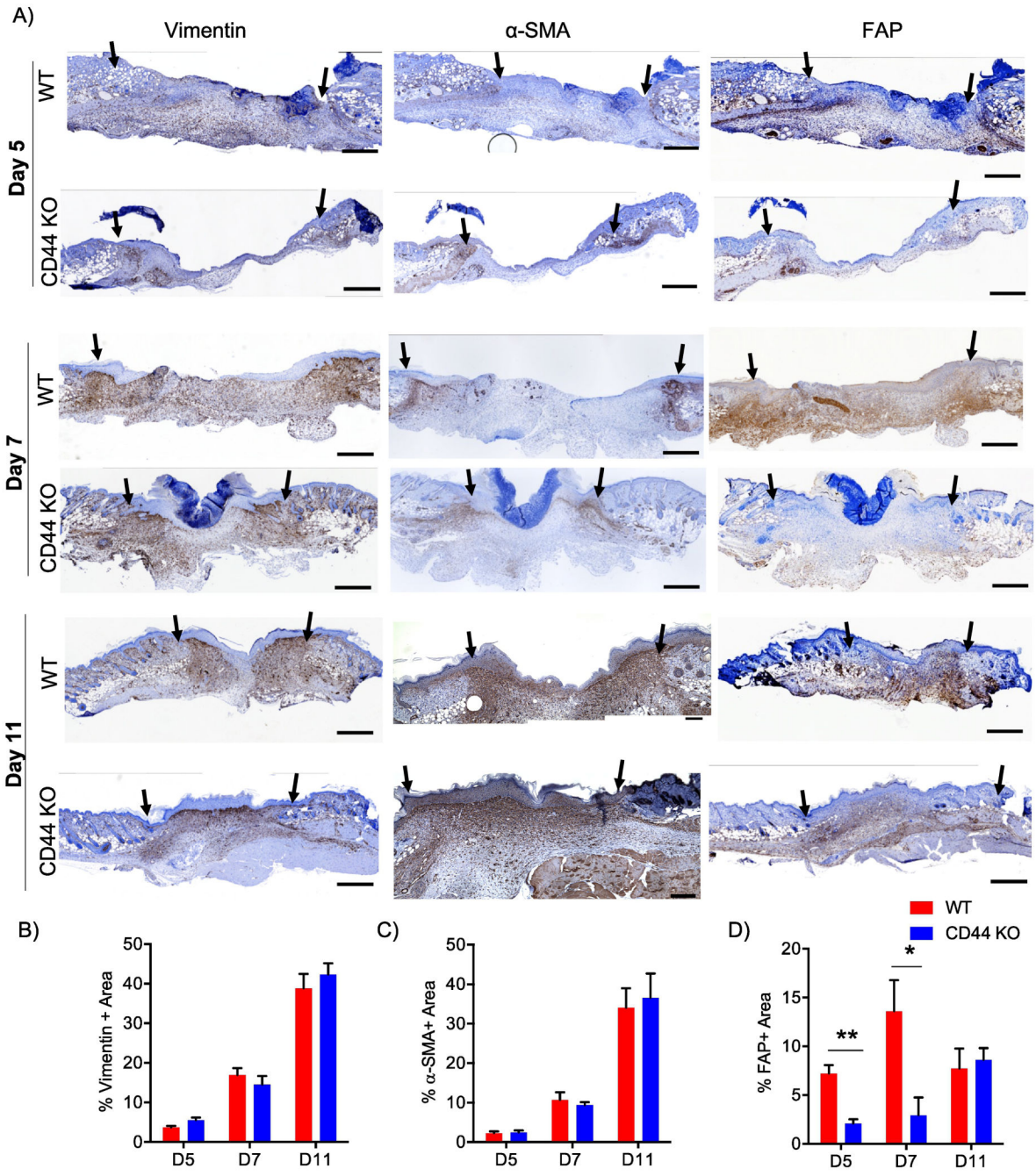

Figure 2. CD44 deficiency attenuates FAP$^+$ fibroblast accumulation during early phases of wound healing.

A) Representative 10x images of vimentin, α-SMA, and FAP IHC images 5 days 7 days and 11 days post-wounding. Black arrows indicate wound edges. Quantification of B) vimentin$^+$ area C) α-SMA$^+$ area and D) FAP$^+$ area normalized to total granulation tissue area, n=6-7 per group. Scale bars = 500¼m. Bar graphs depict mean ± SEM. ** $p < 0.01$ and * $p < 0.05$

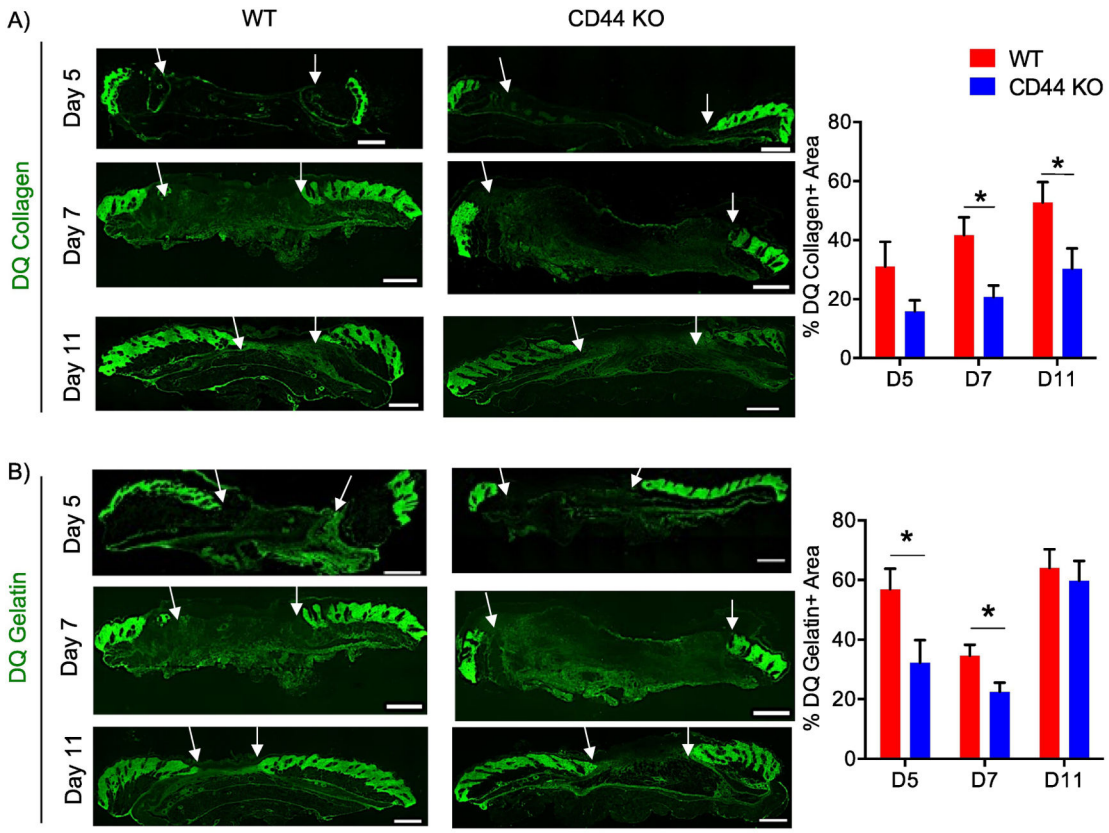

Figure 3. CD44 deficiency reduces collagenolysis during cutaneous wound healing.

A) Representative 20x images of DQ collagen staining of wounds extracted 5, 7, and 11 days post-wounding (left) and quantification of DQ collagen positive area normalized to total granulation tissue area (right), n=6-7 per group. B) Representative 20x images of DQ gelatin staining of wounds extracted 5, 7, and 11 days post-wounding (left) and quantification of DQ gelatin positive area normalized to total granulation tissue area (right), n=6-7 per group. White arrows indicate wound edges. Scale bar = 500μm. Bar graphs depict mean ± SEM. * $p < 0.05$

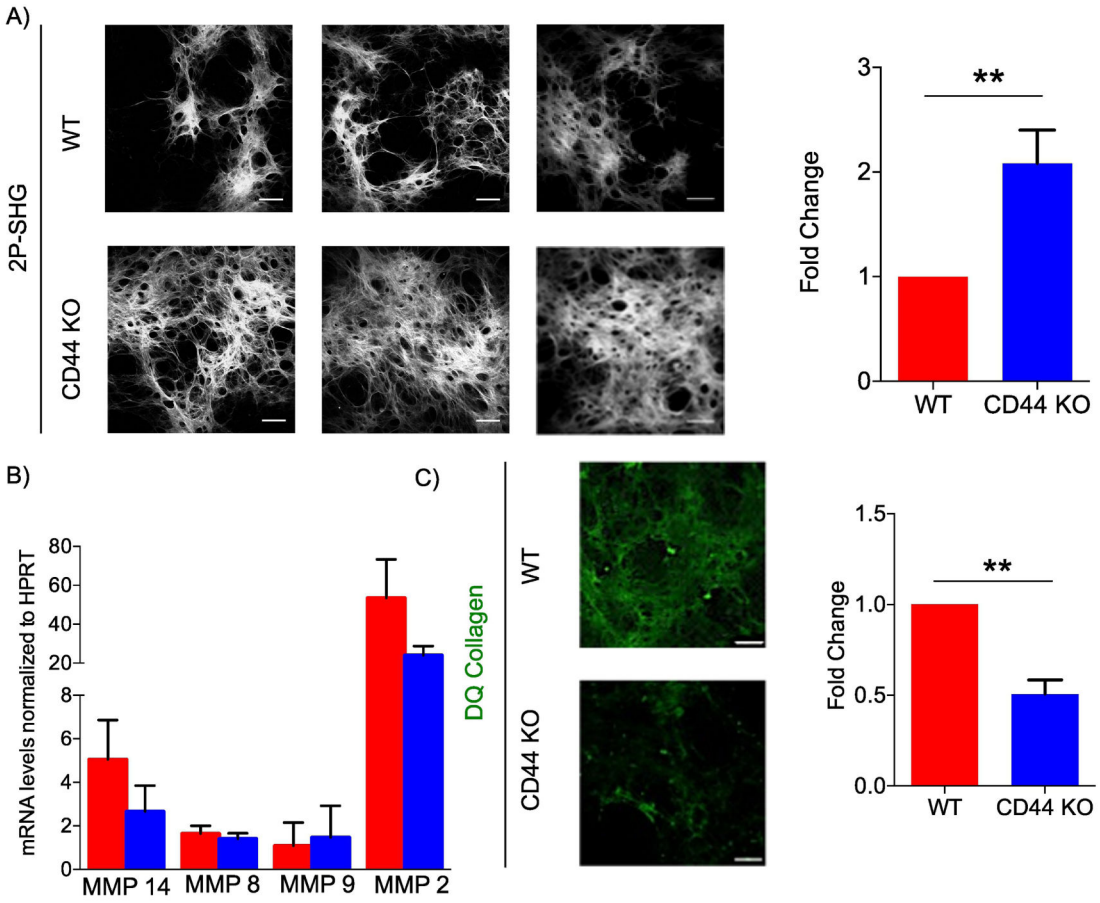

Figure 4. CD44-null fibroblast-derived matrices have increased fibrillar collagen accumulation and reduced MMP activity compared to WT.

A) Representative 2P-SHG images of decellularized matrices derived from WT or CD44-null dermal fibroblasts (left). Scale bars = 200μm. Quantification of SHG positive area. Data combined from 5 independent experiments (right). B) QRT-PCR of Mmp 14, Mmp8, Mmp9, and Mmp 2 mRNA levels in fibroblasts depositing matrices on 8th day of matrix production. Data combined from 4 independent experiments. C) Representative IF images of decellularized matrices derived from WT and CD44-null dermal fibroblasts supplemented with DQ collagen 24 hours prior to decellularization. Data combined from 3 independent experiments. Scale bars =100 μm. Bar graphs depict mean ± SEM. ** $p < 0.01$

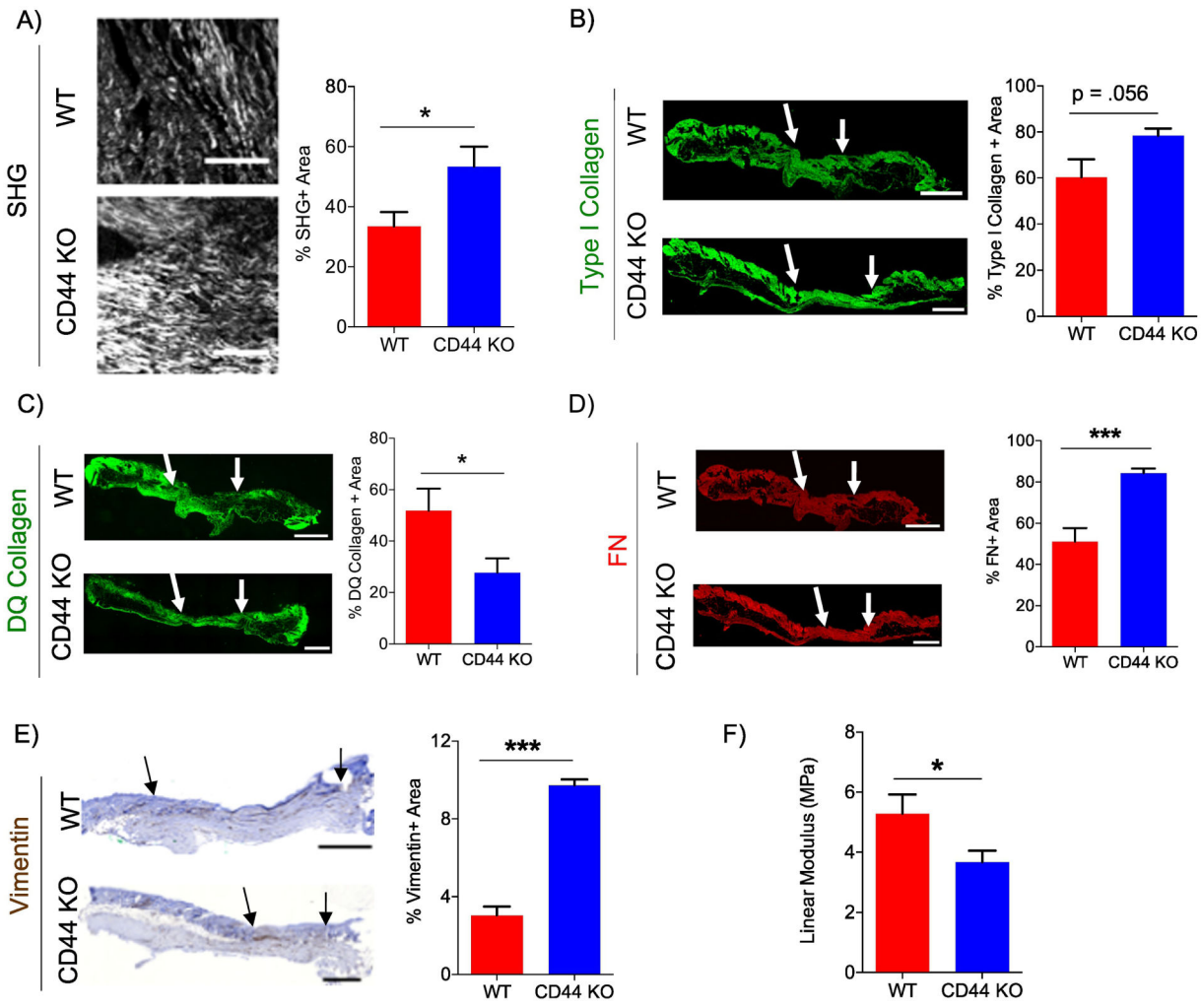

Figure 5. CD44 deficiency increases fibrogenic response and reduces tensile strength in scar tissue.

A) Representative 20x 2P-SHG images of wounds 63 days post-wounding (left). Scale bars = 200μm Quantification of SHG positive area normalized to total scar tissue area (right), n=8 per group. B) Representative 20x type I collagen IF images of wounds 63 days post-wounding (left). Quantification of type I collagen positive area normalized to total scar tissue area (right), n=6 (WT) and 7 (CD44 KO). C) Representative 20x DQ collagen IF images of wounds 63 days post-wounding (left). Quantification of DQ collagen positive area normalized to total scar tissue area (right), n=6 (WT) and 7 (CD44 KO). D) Representative 20x fibronectin IF images of wounds 63 days post-wounding (left). Quantification of FN positive area normalized to total scar tissue area (right), n=6 (WT) and 7 (CD44 KO). E) Representative 10x vimentin IHC of wounds 63 days post-wounding (left). Quantification of vimentin positive area normalized to total scar tissue area (right), n=6 (WT) and 7 (CD44 KO). Arrows indicate wound edges. F) Quantification of Young's Modulus using ramp to failure test of WT and CD44-null wounds 63 days post-wounding, n=8 (WT) and 9 (CD44 KO). Scale bar = 500 μm. Bar graphs depict mean ± SEM. *** $p < 0.001$ * $p < 0.05$

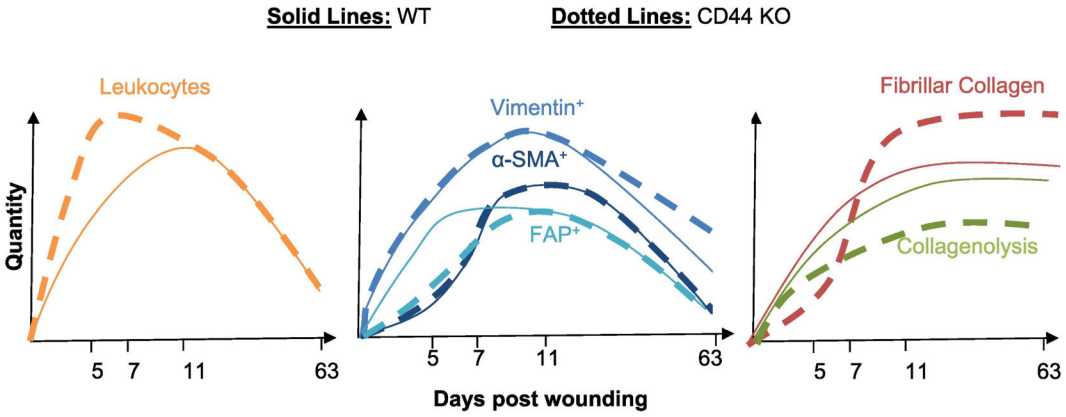

Key Differences in CD44-null wounds compared to WT wounds						
Days post wounding:	Leukocytes	Fibroblasts			Collagenolysis	Fibrillar Collagen
		Vimentin	FAP	α-SMA		
5 & 7	Increased	ND	Decreased	ND	Decreased	Decreased
11	ND	ND	ND	ND	Decreased	Increased
63	ND	Increased	ND	ND	Decreased	Increased

Figure 6: Schematic representation of the impact of CD44 loss on evolution of leukocytes, fibroblasts and fibrillar collagen over the course of wound healing.

During early phases of wound healing (days 5 & 7), CD44 deletion increases the inflammatory response while delaying the fibrotic response. During the tissue remodeling phase of wound healing (days 11 & 63), CD44 deletion decreases collagenolysis, which correlates with increased fibrillar collagen accumulation.